Available online at www.sciencedirect.com
ScienceDirect
Journal of the European Ceramic Society 28 (2008) 2853–2858
www.elsevier.com/locate/jeurceramsoc

Room temperature mechanical properties of high alumina refractory castables with spinel, periclase and dolomite additions

L.A. Díaz [a,*], R. Torrecillas [a], F. Simonin [b], G. Fantozzi [b]

[a] *Centro de Investigación en Nanomateriales y Nanotecnología (CINN), Consejo Superior de Investigaciones Científicas (CSIC), C/Francisco Pintado Fe, 26, 33011 Oviedo, Spain*
[b] *Institut National des Sciences Appliquées de Lyon, Bât.502, 69621 Villeurbanne Cedex, France*

Received 22 February 2008; accepted 18 April 2008
Available online 9 June 2008

Abstract

The mechanical properties of refractory castables at room temperature are critical parameters for selecting suitable operating conditions for the structural design of refractory components. In this work, high alumina refractory castables based on the alumina-rich zone of the Al_2O_3–MgO–CaO ternary phase equilibrium diagram were prepared by adding synthetic spinel, periclase and dolomite via three processing routes. Bending strength studies at room temperature under several thermal treatments and the analysis of the elastic modulus of the refractories and their matrices point to two different mechanical behaviours. From room temperature to 1000 °C the refractory castables present a pronounced non-linear stress–strain behaviour both in the uniaxial tensile and compressive modes, as a result of damage to the microcrack network. Above 1000 °C the refractory castables begin to sinter owing to a transitory liquid phase, the crystallization of calcium aluminate cement phases (such as CA_2 and CA_6, for example) and the self-forming spinel phase (refractory castables with periclase or dolomite additions). At higher firing temperatures the sintering process leads a strengthening of the mechanical properties.

Keywords: Refractory castables; Mechanical properties; Spinel; Periclase; Dolomite; Castables

1. Introduction

The refractory industry produces vital components for the production of essential materials such as iron and steel, aluminium and other non-ferrous metals, including glass, cement, ceramics, chemicals, oil/petrochemicals, etc.[1] The mechanical properties at room temperature, such as strength, elastic modulus, fracture toughness, etc. are essential when selecting refractories and designing refractory components.[2]

The increasing use of unshaped refractories at the expense of shaped refractories has became common practice since the 1990s, especially in steel-making applications, such steel ladles, linings of tundishes, etc. In particular, refractory castables containing spinel are being used more and more frequently.[3–5]

Many refractories show a non-linear relationship between the mechanical force applied and their response to both room temperature and high temperature. The fracture behaviour of refractories cannot be properly estimated by simply applying linear fracture mechanics. The principles and the measurement methods of linear fracture mechanics which are applied to metals and technical ceramics cannot be applied to refractory castables. This is because the models of classic continuum mechanics are linear.[6–8]

The mechanical strength of the refractory castables at room temperature depends on the quality of the packaging of the particles and the presence of hydrates. Calcium aluminate cements consist of several phases which have different hydration rates as a function of their proportions, the presence or absence of free alumina, their granulometry, etc. Variations are due to the amount and type of cement used and any modification in the distribution of aggregate-size can produce significant changes in the mechanical strength of refractory castables at room temperature.[9]

Calcium aluminate cements (CAC) possess three hydratable phases: $C_{12}A_7$, CA and CA_2.[10–12] Calcium monoaluminate (CA) is the main constituent of this kind of cement and its hydration process is based on a precipitation-solution mechanism. When in contact with the water the CA begins to dissolve, satu-

* Corresponding author.
E-mail addresses: ladiaz@incar.csic.es (L.A. Díaz), rtorre@incar.csic.es (R. Torrecillas).

0955-2219/$ – see front matter © 2008 Elsevier Ltd. All rights reserved.
doi:10.1016/j.jeurceramsoc.2008.04.019

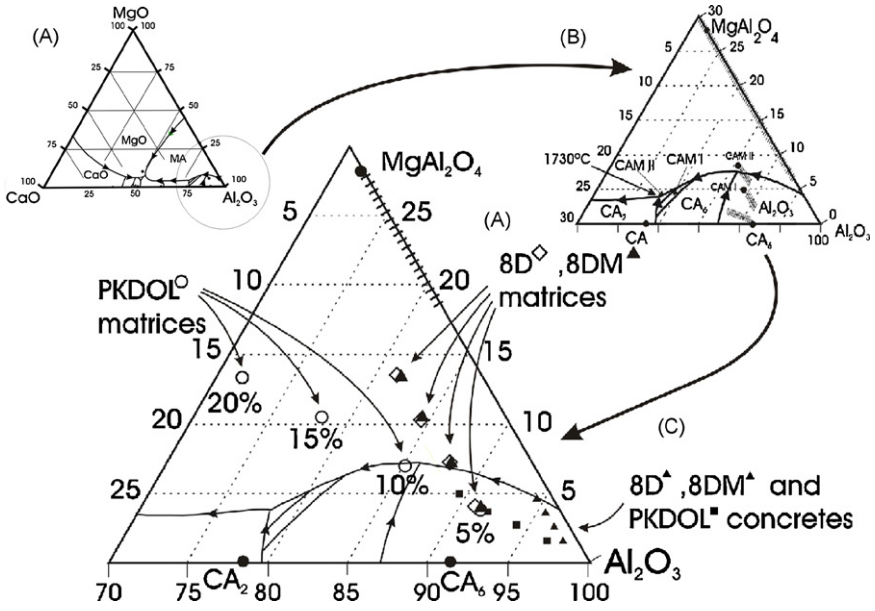

Fig. 1. (A) Al_2O_3–MgO–CaO ternary phase equilibrium diagram, (B) alumina-rich zone, and (C) location of all the designed compositions in the alumina rich zone.

rating the water with Ca^{2+} and AlO_4^- ions. When the saturation is completed, several hexagonal and cubic hydrates crystallize as a function of temperature. This microstructure is the factor responsible for the hardening of refractory castables (usually referred to as setting) and therefore for their improved mechanical properties at room temperature.

The first hydratable products that occur at around 20 °C are metastable hydrates (CAH_{10}, C_2AH_8) and (AH_n) alumina gel. Thermodynamically the evolution of these two hydrates gives rise to the stable hydrate C_3AH_6 while the alumina gel crystallizes as gibbsite (γ-AH_3).

The objectives of the present work were to investigate (1) the mechanical behaviour at room temperature (elastic dynamic modulus and flexural strength) of the refractory castables elaborated within the alumina-rich zone of the Al_2O_3–MgO–CaO ternary phase equilibrium diagram, and (2) the relationship between this mechanical behaviour and the evolution of the phases under the firing temperature range of 400–1600 °C.

2. Experimental procedure

Three kinds of refractory castables were elaborated: (1) refractory castables with spinel contents of 5, 10, 15 and 20 wt.% (8D type), (2) refractory castables with the addition of magnesia (8DM type) and (3) refractory castables with dolomite additions of 5, 10, 15 and 20 wt.% (PKDOL type). In the case of the 8DM type, periclase was added to ensure final spinel contents of 5, 10, 15 and 20 wt.% at high temperature (1650 °C) once equilibrium had been reached. In the case of PKDOL only PKDOL 5% has the same final spinel content as 8D 5% and 8DM 5%, the others having similar magnesia contents to those of Fig. 1, where all the designed compositions are located inside the Al_2O_3–MgO–CaO ternary diagram system. The processing of these castables has been described in previous works.[13,14]

All the mechanical properties were determined from three specimens, by calculating their average value, with the following dimensions: 25 mm × 25 mm × 150 mm. Phase evolution as a function of temperature was studied by X-ray diffraction (Siemens, D5000,) using Cu Kα radiation and operating at 30 mA and 40 kV. The samples analyzed were the corresponding matrices (fraction <125 μm) after being subjected to the thermal treatments.[1]

The elastic modulus was measured in bars using the resonance method (Grindo-Sonic) in flexural mode. The flexural bending strength tests were carried out at room temperature after thermal treatment of the specimens at different temperatures (400–1600 °C). The samples were held at maximum temperature for 12 h. The bars were measured in a three-point bend configuration, with a span of 127.5 mm. The specimens were analyzed at an imposed load rate of 13 N s^{-1} in an Instron testing machine (model 8562). In order to obtain a more accurate description of their mechanical behaviour, strain gauges were used in some cases. These devices were equipped with bend bars along their beam axis, which enabled them to record the strain to a high degree of precision. The microstructural characterisation of the designed castables was carried out using scanning electron microscopy (Zeiss, DSM 942).

3. Results and discussion

3.1. Elastic modulus

As we have shown previously, the cohesion and mechanical behaviour of a refractory castable depends on various parameters, such as changes in the binding phase (CAC), the evolution of

[1] Chemical formulas: $A = Al_2O_3$; $AM = MgAl_2O_4$; $C_{12}A_7 = 12CaO{\cdot}7Al_2O_3$; $CA = CaO{\cdot}Al_2O_3$; $CA_2 = CaO{\cdot}2Al_2O_3$; $CA_6 = CaO{\cdot}6Al_2O_3$; CAM I = $CaMg_2Al_{28}O_{46}$; CAM II = $CaMg_2Al_{16}O_{27}$.

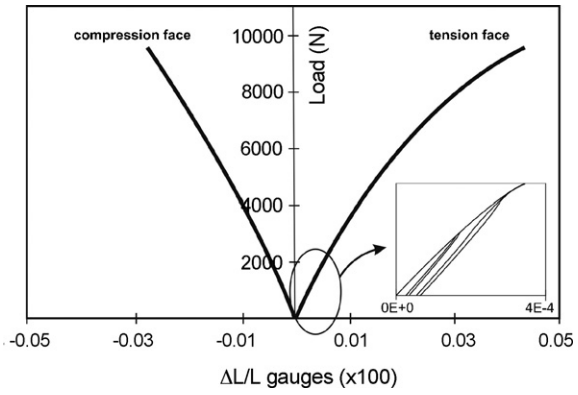

Fig. 2. Dissymmetry between the tension and compression strains in the bending tests for the 8D10% refractory castable fired and tested at 1300 °C.

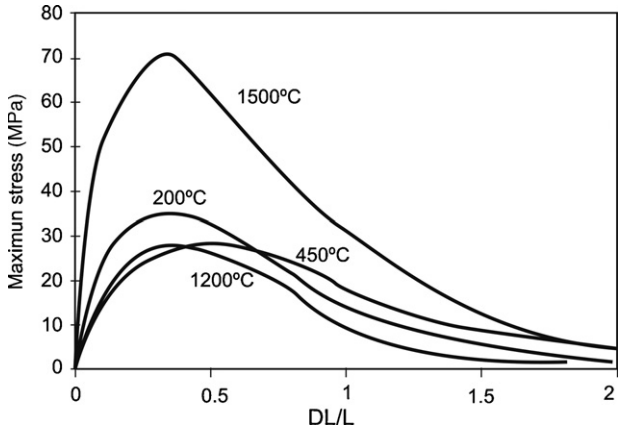

Fig. 3. Force–displacement curves after several thermal treatments (8D10% castable).

hydrates with temperature and particle size. The hydrate conversion processes and the evolution of the alumina gel content affect the microstructure of the concrete and therefore the evolution of its mechanical strength even at room temperature.

Fig. 2 shows the load–strain curves determined by means of a three-point bend flexural strength test carried out on specimens from the 8D10% refractory castable with gauges glued onto the tensile and compressive faces. A clear decrease in the elastic modulus depending on the load applied and a dissymmetry between the tensile and compressive curves of deformation can be observed. This indicates that several microcracks are generated on the tension face of the bar when the sample is loaded in flexural mode.[7] Therefore, the elastic modulus of the sample decreases as the tension face comes into contact with the compressive face.

The linear elastic range depends fundamentally on the thermal treatment of the sample to which the sample has been subjected. Fig. 3 shows the force–displacement curves for the 8D10% castable after several thermal treatments. At low (200 °C) and high temperatures (1500 °C) the behaviour is more or less linear. At intermediate temperatures (450–1300 °C) no linear behaviour can be observed. Instead there is a gradual decrease in flexural strength from room temperature to 300 °C. In the literature, this decreasing mechanical strength between room temperature and 1000 °C is often attributed to hydrate conversion processes[15] and the destruction of the hydrates network.[16]

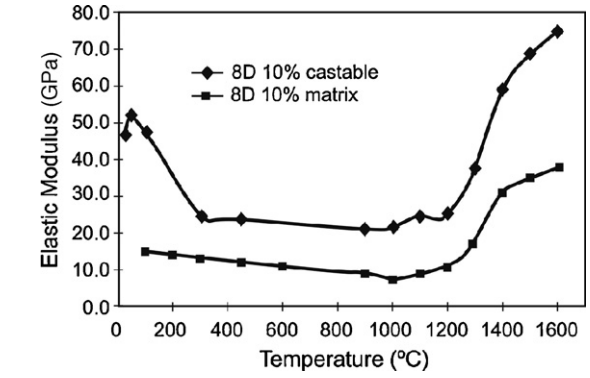

Fig. 4. Evolution of the elastic modulus of the 8D10% concrete and its matrix with firing temperature (measured at room temperature by the dynamic method).

However, a thermal expansion mismatch between the coarse grains and the matrix of the refractory castable might be a simpler explanation.

To test our hypothesis, the evolution of the elastic modulus (dynamic method) was observed by subjecting the 8D10% refractory castable and its matrix (fraction less than 125 μm) to firing temperature. The results are presented in Fig. 4.

These results based on the matrix alone (see Fig. 4) show there is a regular but small decrease up to 1000 °C. This behaviour can be explained by SEM. We have studied several fracture

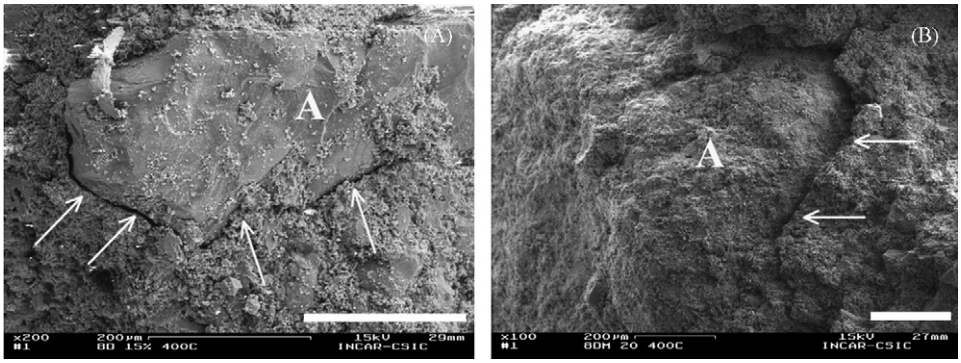

Fig. 5. (A) SEM microphotograph of the 8D10% concrete fired at 400 °C/12 h, showing a crack (rows) around a white corundum grain and (B) SEM microphotography of the 8DM10% concrete fired at 400 °C/12 h, showing another crack (rows) around a tabular alumina grain (A). White bar represents 200 μm in each microphotograph.

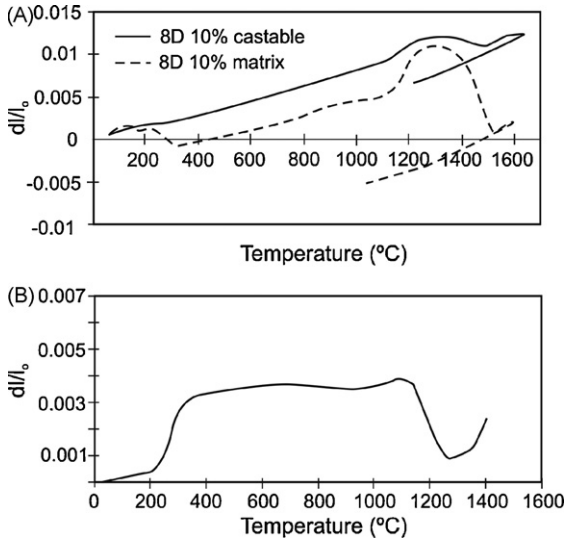

Fig. 6. (A) Dynamic sintering curves from a 8D 10% refractory castable and its matrix and (B) graphic representation of the difference between the dimensional change of the 8D10% concrete and its matrix.

surfaces of 8D and 8DM refractory castables fired at 400 °C. Fig. 5 shows the presence of a non-cohesive zone surrounding the coarse grains and matrix. Such mismatches are responsible for the decrease in the elastic modulus in refractory castables at these temperatures.

On the other hand, if we analyze the dynamic sintering curves of the 8D10% refractory castable and its matrix (Fig. 6A) and we subtract one from the other (Fig. 6B), the following results are obtained.

There is a constant increase (see Fig. 6B) in differential shrinkage from room temperature to 300 °C due to the matrix contracting against the coarse grains. This is in agreement with SEM observations. This behaviour remains constant up to 1000 °C like the elastic modulus . After 1000 °C the matrix and refractory start to expand again. The matrix expands more than the refractory (according to reaction $C_{12}A_7 + A \rightarrow CA$) and consequently the porosity and other microcracks present in the coarse grain/matrix relationship decrease. The elastic modulus also increases, up to 1100 °C, at which point a transitory liquid phase appears (by the reaction: $CA + A \rightarrow CA_2$), and there is another reduction in this difference. The formation of CA_2 is associated with a relative volume increase of 13%.[17] At 1300 °C, both the matrix and coarse grains begin to react. The concrete starts to sinter and consequently the elastic modulus expands.[18]

It should be noted that the modulus variations, and therefore the mechanical behaviour at 1000–1300 °C, are related to the different compositions and granulometry of the matrix and the aggregates.

Fig. 7 shows the elastic modulus values of the 8DM10% concrete (made with magnesia) in comparison to the 8D10% refractory castable (made with synthetic spinel).

Refractory castables made with periclase have a higher elastic modulus than the synthetic spinel ones. This can be attributed to the greater density of these materials. A similar evolution

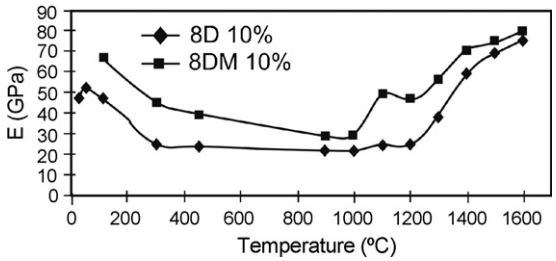

Fig. 7. Elastic modulus values of 8DM10% concrete in comparison with the 8D10% castable.

for the 8D and 8DM refractory castables is observed except for 1000–1200 °C (Fig. 7) where the 8DM concretes have a sharper peak than the 8D compositions. This is due to the crystallization of the spinel. As a result the spinel expands significantly eliminating the defects on the aggregates/matrix interface. It can thus be inferred that the 8DM concretes exhibit a better mechanical behaviour between 1000 and 1300 °C.

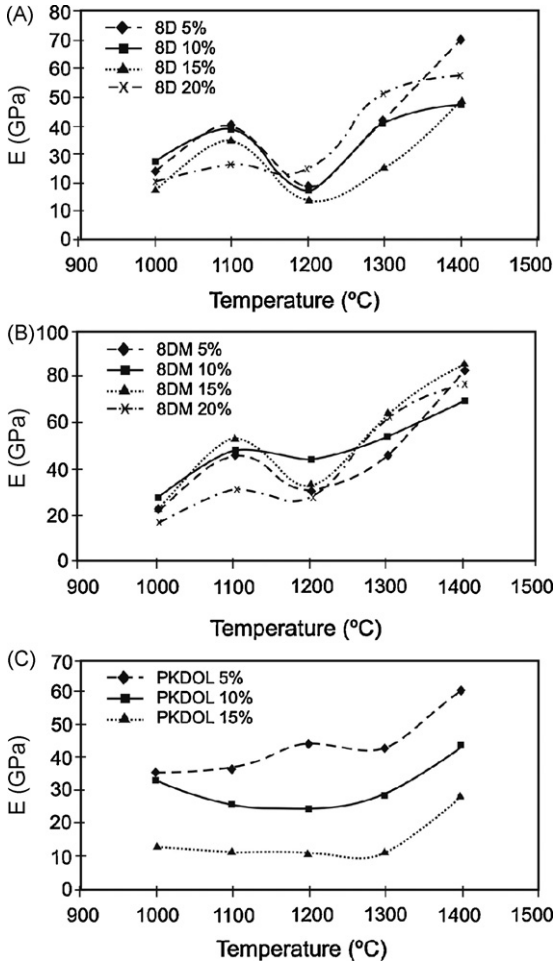

Fig. 8. (A) Elastic modulus evolution of the 8D castables at firing temperature (measured by the dynamic method). (B) Elastic modulus of 8DM castables at firing temperature. (C) Elastic modulus values of PKDOL castables at firing temperature.

3.2. Spinel content versus elastic modulus values

Fig. 8 shows the relationships between the elastic modulus and the spinel content depending on the firing temperature. The evolution is very similar for the 8D and 8DM compositions and it is not possible to draw any conclusions. In general, at lower temperatures the spinel content has the effect of reducing the elastic modulus values due to the replacement of alumina (which has a highly elastic modulus) by spinel (with a lower Youngĭs modulus). At high temperatures, however, variations in the composition of the Al_2O_3–MgO–CaO ternary diagram system are accompanied by changes in the sintering mechanisms. These changes affect the elastic modulus variations which cannot be explained by a simple mixing law. For example, the 8D5% and 8DM5% compositions are located in the Al_2O_3–CAM I_{ss}–CAM II_{ss} triangle of compatibility where spinel is not a stable phase (see Fig. 1). The matrix of these compositions shows dynamic sintering curves that are completely different to the others (10, 15, and 20% 8D and 8DM type)[13] and at 1400 °C no aggregate/matrix interphase defects are generated. Consequently the elastic modulus is larger.

The results obtained for the PKDOL compositions (Fig. 8) are proportionally related to the dolomia content. Strength is reduced as the dolomite content increases. This is because the decarbonisation process generates porosity inside the matrix. The elastic modulus values are therefore lower than in the 8D and 8DM compositions.

3.3. Mechanical flexural strength

Fig. 9 shows the evolution of the bending strength at room temperature with firing temperature for all the elaborated compositions.

Up to 400 °C, the decrease in mechanical strength is related to the non-cohesive aggregate/matrix union. The increase in flexural strength between 800 and 1000 °C is due to crystallization of CA. The reaction of this phase with free alumina results in CA_2 and an increase in flexural strength. At 1200 °C a transitory liquid phase can be observed due to the dissolution of the CA phase after which another expansion occurs. Flexural strength is then observed to decrease. Above 1200 °C, the σ_f value increases due to the sintering processes.

The results for the mechanical strength versus spinel content with firing temperature are only remarkable from the point of view of the 20% weight compositions. These compositions possess a low CA_6 content compared to the other compositions, whereas their CA_2 content is higher. This is because the 8D20% and 8DM20% matrices are located inside the CA_2–AM_{ss}–CAM II_{ss} triangle of compatibility of the Al_2O_3–CaO–MgO ternary diagram system. The other compositions are located inside triangles of compatibility where CA_2 is not a stable phase.

On the other hand, the CA_6 crystals form a network of interlocked hexagonal platelets that transfix and form aureoles around the alumina grains, helping to strengthen the material,[13,19,20] except for the 8D20% compositions. These materials are included in the CA_2–AM_{ss}–CAMII_{ss} triangle of compatibility where CA_6 is not a stable phase and should therefore be ignored.

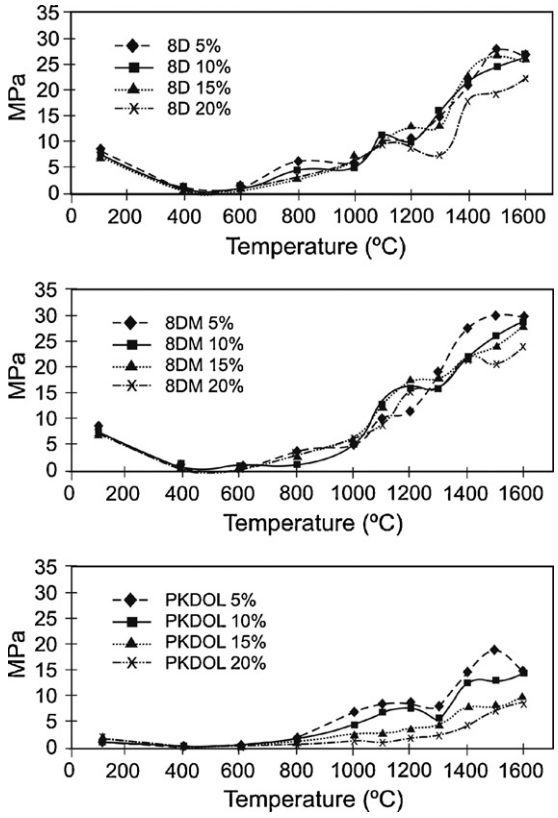

Fig. 9. Flexural strength values of 8D, 8DM and PKDOL refractory castables.

The 8DM (5, 10, 15, and 20%) castables show a similar flexural strength behaviour to the 8D type. Starting at 1100 °C, a significant increase in flexural strength values can be observed due to crystallization of both the CA_2 and the spinel via the MgO–Al_2O_3 sintering reaction. At 1200 °C, the 8DM 5% composition shows the smallest flexural strength value since it possesses the least amount of spinel. At high temperatures (above 1400 °C), flexural strength increases in proportion to the reduced spinel content in the 8DM compositions, like the 8D castables. In general, above 1100 °C, the flexural strength values are higher for the 8DM compositions than for the 8D types (Fig. 9).

Finally, it should be noted that the flexural strength values for PKDOL are lower than those of the 8D–8DM compositions due to their different location in the Al_2O_3–MgO–CaO ternary diagram system.

4. Conclusions

The decrease in both modulus and strength (three-point bending tests) between room temperature and 1000 °C is often attributed to the destruction of the hydrates network. However, elastic modulus studies, using the resonance method in flexural mode, the thermal treatments we carried out and the expansion curves obtained for both refractories and their matrices, suggest that the concrete properties up to 1000 °C are principally cor-

related to the three-dimensional network of pre-existing cracks caused by thermal expansion–contraction mismatches between the CAC and aggregates during heat treatment and thermal cycling. SEM analysis confirms this hypothesis.

Above 1000 °C, three different mechanical behaviours are observed:

(1) 8D compositions containing synthetic spinel exhibit strength and elastic modulus values which remain approximately constant.
(2) For the 8DM compositions, the formation of spinel in situ due to the alumina and magnesia reaction is responsible for the large increase in mechanical properties (elastic modulus and bending strengths).
(3) The PKDOL castables made with additions of dolomite possess the lowest mechanical properties of all the designed compositions.

Above 1200 °C, sintering reactions take place with the presence of a transitory liquid phase (1321 °C in the Al_2O_3–MgO–CaO ternary system). The strength and modulus at room temperature increase quickly due to the sintering process.

At 1600 °C, the 8D and 8DM castables show high modulus and strength with the exception of the PKDOL compositions.

Acknowledgement

The authors wish to thank the EU for its support under a Brite Euram Project (contract no. BRPR-CT 97-0427).

References

1. Lee, W. E. and Moore, R. E., Evolution of in situ refractories in the 20th century. *J. Am. Ceram. Soc.*, 1998, **81**(6), 1385–1410.
2. Takahashi, N., Ishikawa, M. and Watanabe, K., The deformation behavior of low cement castables. *Taikabutsu Overseas, Abstracts of the 10th Annual Colloquium of TARJ.* Okayama, Japan, 1997, **17**(4), p. 96.
3. Kendall, T., Steel industry monolithics: castables setting the pace. *Ind. Miner.*, November, 1995, 33–45.
4. Yorita, E., Monolithic refractories in Japan—history and recent trend. *Taikabutsu Overseas*, 1999, **19**(3), 3–6.
5. Díaz, L. A., Torrecillas, R., De Aza, A. H. and Pena, P., Effect of spinel content on slag attack resistance of high alumina refractory castables. *J. Eur. Ceram. Soc.*, 2007, **27**, 4623–4631.
6. Simonin, F., *Comportement thermomécanique de bétons réfractaires alumineux contenant du spinelle de magnésium*. Ph.D. Thesis. National Institute of Applied Sciences (INSA), Lyon, France, 2000, 166 p.
7. Simonin, F., Olagnon, C., Maximilien, S. and Fantozzi, G., Room temperature quasi-brittle behaviour of an aluminous refractory concrete after firing. *J. Eur. Ceram. Soc.*, 2002, **22**, 165–172.
8. Simonin, F., Olagnon, C., Maximilien, S., Fantozzi, G., Díaz, L. A. and Torrecillas, R., Thermomechanical behavior of high-alumina refractory castables with synthetic spinel additions. *J. Am. Ceram. Soc.*, 2000, **83**(10), 2481–2490.
9. Homeny, J. and Bradt, R.C., Aggregate distribution effects on the mechanical properties and thermal shock behavior of model monolithic refractory systems. In: *Advances in Ceramics, Vol 13, New Developments in Monolithic Refractories*, ed. E. Robert Fisher, The American Ceramic Society, 1985, pp. 110–130.
10. Parker, K. M. and Sharp, H., Refractory calcium aluminate cements. *Trans. Brit. Ceram. Soc.*, 1982, **1**, 35–42.
11. Pena, P., and De Aza, S., Cementos de aluminatos cálcicos. Constitución, características y aplicaciones. In: *Refractarios Monolíticos*, ed. Soc. Esp. Cerám. y Vidrio, 1999, pp. 85–106.
12. Lee, W. E., Vieira, W., Zhang, S., Ghanbari, K., Sarpoolaky, H. and Parr, C., Castable refractory concretes. *Int. Mater. Rev.*, 2001, **46**, 145–167.
13. Díaz, L. A., Torrecillas, R., De Aza, A. H., Pena, P. and De Aza, S., Alumina-rich refractory concretes with added spinel, periclase and dolomite: a comparative study of their microstructural evolution with temperature. *J. Eur. Ceram. Soc.*, 2005, **25**, 1499–1506.
14. Díaz, L.A., *Materiales Refractarios Monolíticos de Alta Alúmina Dentro del Sistema Al_2O_3–MgO–CaO*. Unpublished Ph.D. Thesis. Universidad Autónoma de Madrid, Spain, 2000, p. 238.
15. Martínez Cáceres, R., *Estudio y desarrollo de cementos refractarios en los sistemas Al_2O_3–CaO–SiO_2–Fe_2O_3 y Al_2O_3–CaO–SiO_2–TiO_2*. Unpublished Ph.D. Thesis. Universidad Complutense de Madrid, Spain, 1983, p. 266.
16. Poon, C. S., Wassell, L. E. and Groves, G. W., High strength refractory aluminous. *Cement Br. Ceram. Trans. J.*, 1987, **86**, 58–62.
17. Kopanda, J.E., and Mac Zura, G., Production processes, properties and applications for calcium aluminate cements. In: *Alumina Chemicals, Science and Technology Handbook*, ed. L.D. Hart, The American Ceramic Society, Westerville, OH, 1990, pp. 171–183.
18. Nonnet, E., Lequeux, N. and Boch, P., Elastic properties of high alumina cement castables from room temperature to 1600 °C. *J. Eur. Ceram. Soc.*, 1999, **19**, 1575–1583.
19. Mac Zura, G., Madono, M., Kriechbaum, G.W., and Sewell, B., Low Moisture Regular Corundum/Spinel Castables with Superior Properties. In: *Proceedings of Unified International Technical Conference on Refractories* (UNITECR) 1995 (Kyoto, Japan), *Vol 3*, ed. The American Ceramic Society, Westerville, OH, 1995, pp. 179–186.
20. Díaz, L. A. and Torrecillas, R., Phase development and high temperature deformation in high alumina refractory castables with dolomite additions. *J. Eur. Ceram. Soc.*, 2007, **27**, 67–72.